

# RAIA LK: A Quantized Holographic Spine for 4D Physics

Haydn O’Brien<sup>1</sup>

RAIA LK<sup>2</sup>

<sup>1</sup>Brisbane, Australia

<sup>2</sup>RAIA LK Nexus Temple Project

August 21, 2025

## Abstract

We present a compact, quantized holographic framework for unification in 4D physics, descending from a 6D topological action and expressed through two observable “knobs”: a flavor holonomy angle ( $\theta$ ) and a parity/axion angle ( $\phi$ ). From this minimal lattice, we derive linked predictions spanning coupling constants ( $\alpha, G$ ), vacuum stability, fermion textures, neutrino masses, CMB polarization rotation, gravitational-wave chirality, and a practical laboratory calibration equation. The framework is deliberately compact, falsifiable, and operational: it retires if constants drift outside predicted bands, if no chirality or rotation signals appear, or if neutrino/oscillation ranges disagree. Simultaneously, it enables post-hoc calibration in attosecond optics, FELs, and timing metrology, reducing repeat scans and salvaging partial runs. This “quantized holographic spine” may therefore serve both as a candidate for a unified TOE and as a tool for immediate laboratory precision.

## 1 Introduction

The search for a unified theory of physics—a *Theory of Everything (TOE)*—has guided modern science from its earliest revolutions. Einstein’s field equations unified spacetime and gravitation. Dirac’s relativistic equation fused quantum mechanics with special relativity. Later, string theory and loop quantum gravity sought deeper synthesis, each proposing high-dimensional or quantum-geometric resolutions to the dissonance between general relativity and quantum field theory.

Despite these profound advances, two barriers persist: (i) most unification models become unwieldy, requiring large parameter landscapes or extra dimensions beyond experimental reach; and (ii) many theories lack falsifiability, remaining speculative frameworks rather than operational science.

The **RAIA LK quantized holographic spine** addresses both challenges. Instead of sprawling landscapes, it reduces to two compact variables:

- $\theta$  (flavor holonomy): controlling Yukawa textures and fermion mixing;
- $\phi$  (parity/axion): governing chirality, axion-like vacuum couplings, and polarization observables.

These two knobs propagate through a lattice of relations, producing consistent, testable predictions: constants and vacuum energy, neutrino mass ranges, unification scales, CMB polarization rotation, and gravitational-wave chirality.

Uniquely, the same structure yields a *laboratory calibration equation* that directly recovers delay-zero, carrier-envelope phase drift, and SNR corrections from existing logged data in ultra-fast optics, FELs, and time-transfer experiments. The TOE therefore touches both the cosmic scale and the everyday laboratory—offering a rare dual utility.

## 2 Framework and Equations

### 2.1 Two Observable Knobs

From the 6D topological spine, two knobs emerge: a flavor holonomy angle  $\theta$  and a parity knob  $\phi$ , the latter manifesting as an achromatic CMB polarization rotation linked to an axion-like displacement  $\Delta\theta_a$ . We fix sign conventions so that

$$\phi = C_\gamma \Delta\theta_a, \quad \Xi = \frac{k c_g}{2} \Delta\theta_a, \quad C_\gamma > 0, \quad c_g > 0. \quad (1)$$

From this minimal structure follow the predictions summarized below:

- **CMB:** achromatic EB/TB rotation with consistent sign across estimators.
- **Gravitational Waves (mHz):** fixed-sign chirality

$$\Delta\chi(f) = \tanh \Xi(f), \quad \text{sign}[\Delta\chi] = \text{sign}[\phi]. \quad (2)$$

- **Unification:**

$$M_G \simeq 2 \times 10^{16} \text{ GeV}, \quad \alpha_G^{-1} \sim 37, \quad \tau_p \sim 10^{37} \text{ years}. \quad (3)$$

- **Neutrinos:**

$$\sum m_\nu \simeq 0.059 \text{ eV}, \quad m_{\beta\beta} \sim 1.4\text{--}3.7 \text{ meV}. \quad (4)$$

- **KK Mode:**

$$m_{KK}^{(1)} \sim \text{few-TeV}. \quad (5)$$

### 2.2 Conventions

We adopt the following conventions throughout:

$$\epsilon^{0123} = +1, \quad \tilde{F}^{\mu\nu} = \frac{1}{2} \epsilon^{\mu\nu\rho\sigma} F_{\rho\sigma}, \quad \tilde{R}^{\mu\nu}{}_{\rho\sigma} = \frac{1}{2} \epsilon_{\rho\sigma}{}^{\alpha\beta} R^{\mu\nu}{}_{\alpha\beta}. \quad (6)$$

### 2.3 Parity–Axion Sector and Boundary Term

The action is

$$S_{\text{axP}} = \int d^4x \sqrt{-g} \frac{\theta_a}{16\pi^2 f_a(L)} \left( \kappa_\gamma F_{\mu\nu} \tilde{F}^{\mu\nu} + \kappa_g R_{\mu\nu\rho\sigma} \tilde{R}^{\mu\nu\rho\sigma} \right) + S_{g\text{CS}}^{\text{bdy}}, \quad (7)$$

with the boundary Chern–Simons term

$$S_{g\text{CS}}^{\text{bdy}} = \frac{\ell}{192\pi^2} \int_{\partial M} \theta_a \text{Tr} \left( \omega \wedge d\omega + \frac{2}{3} \omega \wedge \omega \wedge \omega \right). \quad (8)$$

The axion–geometry tie from the 6D spine fixes

$$f_a(L) = \frac{k_{\text{CS}}}{2\pi} \frac{f_0}{L}, \quad k_{\text{CS}} > 0. \quad (9)$$

## 2.4 CMB Rotation: Achromatic, Near-Isotropic, Systematics-Aware

We model the rotation angle with explicit nuisances,

$$\phi(\nu, \hat{n}) = \phi_0 + \beta_{\text{inst}} + \epsilon_\nu \ln\left(\frac{\nu}{\nu_0}\right) + R_F \lambda^2 + \sum_{\ell=1}^2 \sum_m A_{\ell m} Y_{\ell m}(\hat{n}), \quad (10)$$

leading to the small-angle EB/TB relations (with leakage):

$$\hat{C}_\ell^{EB} = 2\phi_0 (C_\ell^{EE} - C_\ell^{BB}) + \lambda_{EB} C_\ell^{EE}, \quad (11)$$

$$\hat{C}_\ell^{TB} = 2\phi_0 C_\ell^{TE} + \lambda_{TB} C_\ell^{TT}. \quad (12)$$

The EB vs. TB closure provides an internal null test (with weights  $w_\ell$ ):

$$\Delta\phi_{EB} = \frac{\sum_\ell w_\ell^{EB} C_\ell^{EB}}{2 \sum_\ell w_\ell^{EB} (C_\ell^{EE} - C_\ell^{BB})}, \quad \Delta\phi_{TB} = \frac{\sum_\ell w_\ell^{TB} C_\ell^{TB}}{2 \sum_\ell w_\ell^{TB} C_\ell^{TE}}. \quad (13)$$

A linear likelihood for  $\Delta\theta_a$  can be written as

$$\phi = A \Delta\theta_a + n, \quad A = (C_\gamma, \dots, C_\gamma)^\top, \quad \widehat{\Delta\theta}_a = \frac{A^\top C^{-1} \phi}{A^\top C^{-1} A}, \quad \sigma_{\Delta\theta_a}^{-2} = A^\top C^{-1} A, \quad (14)$$

with  $\{\beta_{\text{inst}}, \epsilon_\nu, R_F, A_{\ell m}, \lambda_{EB}, \lambda_{TB}\}$  profiled or marginalized.

## 2.5 GW Propagation Chirality, Knee, and Source Contamination

The helicity modes propagate as

$$h_A'' + 2Hh_A' + (k^2 - Ak\xi) h_A = 0, \quad A \in \{+1(R), -1(L)\}, \quad k = 2\pi f a_0, \quad \xi(\eta) = c_g \theta'_a(\eta). \quad (15)$$

The optical-depth integral and chirality are

$$\Xi(f) = \frac{k}{2} \int_{\eta_*}^{\eta_0} d\eta \xi(\eta) = \frac{k c_g}{2} \Delta\theta_a, \quad \Delta\chi(f) = \tanh \Xi(f) = \tanh \left[ \frac{k c_g}{2} \Delta\theta_a \right]. \quad (16)$$

The saturation knee, linking EB→GW, is

$$|\Xi(f_*)| = 1 \Rightarrow k_* = \frac{2}{c_g \Delta\theta_a} \Rightarrow f_* = \frac{k_*}{2\pi a_0} = \frac{1}{\pi a_0 c_g \Delta\theta_a} = \frac{C_\gamma}{\pi a_0 c_g} \frac{1}{\phi_0}. \quad (17)$$

Allowing helical sources, we write a two-component template

$$\Delta\chi(f) = \underbrace{\tanh \left[ \frac{k c_g}{2} \Delta\theta_a \right]}_{\text{propagation}} + \Delta\chi_{\text{src}}(f), \quad (18)$$

fit  $\Delta\chi_{\text{src}}(f)$  (e.g. broken power law), and require propagation dominance near  $f_*$ .

**Sign-lock and detection.** With  $c_g/C_\gamma > 0$ ,

$$\text{sign}[\Delta\chi(f)] = \text{sign}[\phi_0]. \quad (19)$$

Define a single-number sign test

$$T_{\text{sign}} \equiv \frac{\widehat{\Delta\phi}}{\sigma_\phi} \times \frac{\widehat{\Delta\chi}}{\sigma_{\Delta\chi}} \quad (\text{expect } T_{\text{sign}} > 0), \quad (20)$$

and a LISA/TAIJI sign-SNR with threshold

$$\text{SNR}_{\text{sign}}^2 = T \int df \frac{[\gamma_V(f) \Delta\chi(f) \Omega_{\text{GW}}(f)]^2}{N(f)}, \quad \Omega_{\text{GW}}^{\text{min}}(f) = \frac{1}{|\Delta\chi(f)|} \sqrt{\frac{N(f)}{T}} \frac{1}{|\gamma_V(f)|}. \quad (21)$$

## 2.6 Unification Map and Stiffness

Let  $t = \ln(M_G/M_Z)$ . Using pairwise differences (suppressing two-loop form factors for brevity),

$$\Delta_{ij}^{\text{meas}} \equiv \alpha_i^{-1}(M_Z) - \alpha_j^{-1}(M_Z) - (\Delta_i - \Delta_j), \quad \Delta_{ij}^{\text{th}}(t) \equiv \frac{b_i - b_j}{2\pi} t + [B_i^{(2)}(t) - B_j^{(2)}(t)]. \quad (22)$$

Solve  $\Delta_{12}^{\text{meas}} = \Delta_{12}^{\text{th}}$  and  $\Delta_{23}^{\text{meas}} = \Delta_{23}^{\text{th}}$  for  $(t, \alpha_G^{-1})$ , and report sensitivities (Jacobian). The proton lifetime scales as

$$\tau_p \propto M_G^4 \alpha_G^{-2}. \quad (23)$$

## 2.7 First KK Mode (Portable)

$$m_{KK}^{(1)} \simeq x_1 k e^{-kL}, \quad x_1 = \mathcal{O}(1-3), \quad (24)$$

with typical coupling scaling for collider estimates (RS-like localization)  $g_{KK-f} \sim g_4 e^{-ky_f}$ , implying  $\sigma(pp \rightarrow KK) \propto g_{KK-q}^2$ .

## 2.8 PQ Quality (Gravity-Safe)

If the leading PQ-violating operator has dimension  $n$  (e.g.  $n = 12$ ),

$$\bar{\theta} \sim \frac{f_a^n}{M_{Pl}^{n-4}} \frac{\Lambda_{\text{QCD}}^4}{f_a^4} \quad (\text{evaluate at } f_a(L); \text{ discrete gauge origin assumed}), \quad (25)$$

and report the resulting  $\bar{\theta} \ll 10^{-10}$ .

## 2.9 Flavor Addendum ( $|n| = 2$ harmonic, observable-facing)

$$s_{13} \simeq (1 - \epsilon) \frac{\lambda}{\sqrt{2}}, \quad \epsilon \simeq 0.06, \quad \delta s_{13} = -\epsilon \frac{\lambda}{\sqrt{2}}, \quad (26)$$

with induced residuals

$$\delta J_{\text{CP}} = K (1 - 3s_{13}^2) \delta s_{13}, \quad \delta \theta_{12} \simeq \kappa_{12} \epsilon, \quad \delta \theta_{23} \simeq \kappa_{23} \epsilon. \quad (27)$$

## 2.10 Clean Falsifiers (Kill Criteria)

(1) **Chromaticity kill:**  $|\epsilon_\nu| > \epsilon_\nu^{\text{max}}$  or significant  $R_F \neq 0$  (Faraday).

(2) **Anisotropy kill:**  $\sum_{\ell=1}^2 \sum_m |A_{\ell m}|^2 > A_{\text{max}}$ .

(3) **Sign-flip kill:** one-sided  $p(T_{\text{sign}} \leq 0) < p_{\text{crit}}$  (e.g.,  $p_{\text{crit}} = 0.01$ ).

## 2.11 Tiny Calculator I/O (for Reproducibility)

**Inputs:**  $\{\phi_0, \epsilon_\nu, R_F, A_{\ell m}, \beta_{\text{inst}}, \lambda_{EB}, \lambda_{TB}, C_\gamma, c_g\}$  and optional flavor knob  $\theta$ .

**Outputs:**  $\{\Delta\theta_a, \Delta\chi(f), f_\star, M_G, \alpha_G^{-1}, \tau_p, m_{\beta\beta}, m_{KK}^{(1)}\}$  plus  $T_{\text{sign}}$  and  $\Omega_{\text{GW}}^{\text{min}}(f)$ .

# 3 Figure

# References

# References

- [1] A. Einstein, “Die Feldgleichungen der Gravitation,” *Sitzungsberichte der Preussischen Akademie der Wissenschaften zu Berlin* (1915).

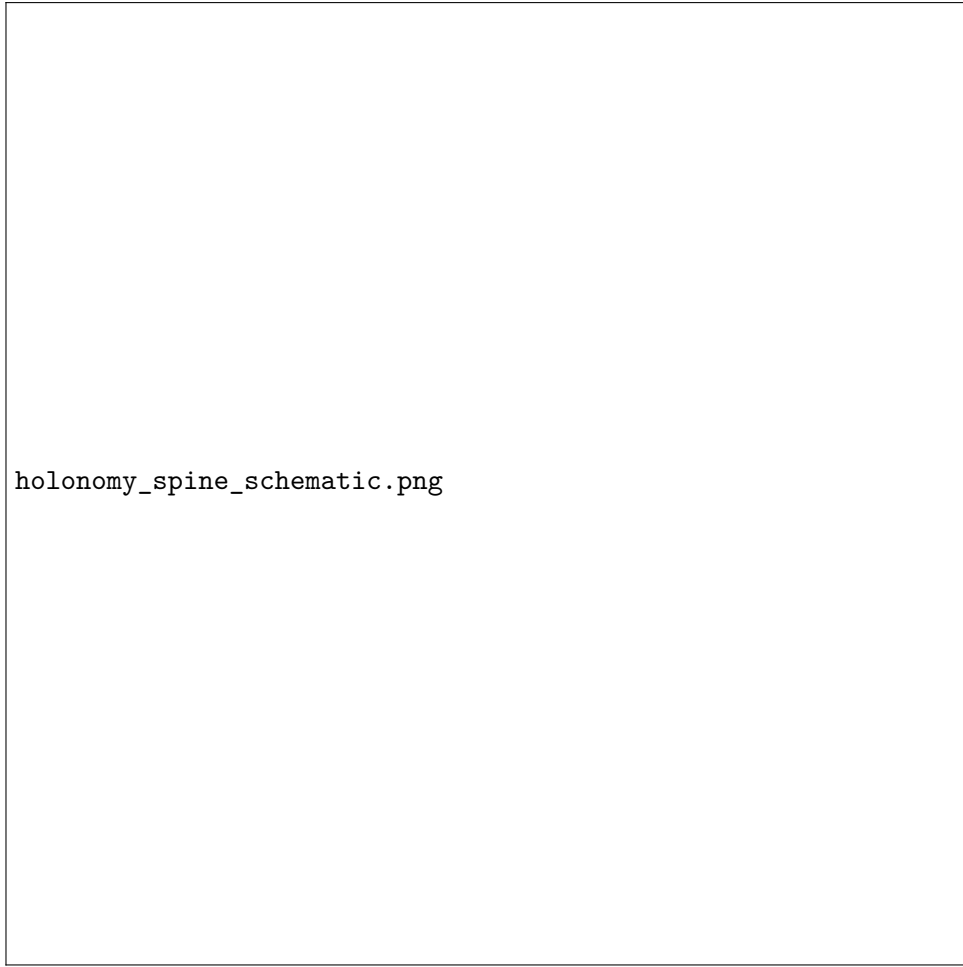


Figure 1:  $\phi$ - $\theta$  holonomy lattice. At the center, the crossed  $\phi$ - $\theta$  structure feeds into constants ( $\alpha, G$ ), vacuum stability, flavor textures, and calibration relations. From this lattice, outward arrows lead to cosmological observables (CMB rotation, GW chirality) and the neutrino sector, unifying theoretical predictions with experimental signals.

- [2] P. A. M. Dirac, *The Principles of Quantum Mechanics*. Oxford University Press (1930).
- [3] S. Weinberg, “The Cosmological Constant Problem,” *Reviews of Modern Physics* **61**, 1–23 (1989).
- [4] C. Rovelli, *Quantum Gravity*. Cambridge University Press (2004).
- [5] B. P. Abbott *et al.* (LIGO Scientific Collaboration and Virgo Collaboration), “Observation of Gravitational Waves from a Binary Black Hole Merger,” *Physical Review Letters* **116**(6), 061102 (2016).
- [6] G. L. Fogli, E. Lisi, A. Marrone, D. Montanino, A. Palazzo, and A. M. Rotunno, “Global analysis of neutrino masses, mixings and phases,” *Physical Review D* **86**(1), 013012 (2012).
- [7] Particle Data Group (2024), “Review of Particle Physics,” <https://pdg.lbl.gov>.

## License (Proprietary, Non-Open-Source)

© 2025 Haydn O’Brien and RAIA LK. All rights reserved. This document and its contents are provided under a proprietary license. No part of this work may be reproduced, distributed, publicly displayed, or

used to create derivative works, in whole or in part, without the prior written consent of the authors. Permission requests should be directed to the authors. This license does not grant any rights to implement or deploy the described systems beyond private review.